

## Structural properties and mechanical stability of monoclinic lithium disilicate

Yohandys A. Zulueta\*\*,1,2, James A. Dawson<sup>3</sup>, Mathy Froeyen<sup>4</sup>, and Minh Tho Nguyen\*,<sup>2</sup>

- <sup>1</sup> Departamento de Física, Facultad de Ciencias Naturales, Universidad de Oriente, CP-90500, Santiago de Cuba, Cuba
- <sup>2</sup> Department of Chemistry, KU Leuven, Celestijnenlaan 200F, B-3001 Leuven, Belgium
- <sup>3</sup> Department of Chemistry, University of Bath, Bath BA2 7AY, UK
- <sup>4</sup> Department of Pharmaceutical and Pharmacological Sciences, Medicinal Chemistry, Rega Institute for Medical Research, KU Leuven, B-3000 Leuven, Belgium

Received 21 March 2017, revised 27 April 2017, accepted 24 May 2017 Published online 14 June 2017

**Keywords** density functional theory, Li<sub>2</sub>Si<sub>2</sub>O<sub>5</sub>, monoclinic, silicate glass ceramics

The structural, electronic and mechanical properties of monoclinic  $\text{Li}_2\text{Si}_2\text{O}_5$  are explored using density functional theory. Different exchange–correlation functionals are considered and the results are correlated to experimental data. The calculated electronic band structure and density of states indicate that monoclinic  $\text{Li}_2\text{Si}_2\text{O}_5$  has an insulating character

with an indirect band gap of 4.98 eV. Elastic stiffness coefficients and the bulk, shear and Young's moduli are also calculated. Our calculations predict that  ${\rm Li_2Si_2O_5}$  is a ductile compound. We show that monoclinic  ${\rm Li_2Si_2O_5}$  behaves as a specially orthotropic material, meaning that the structure can be masked by the orthorhombic form.

© 2017 WILEY-VCH Verlag GmbH & Co. KGaA, Weinheim

**1 Introduction** Lithium silicates are present as important phases in silicate glass ceramics [1–4] and are of research interest due to their technological applications in lithium-ion batteries [2], fast-ion conductors [1, 2],  $CO_2$  adsorption [3], waveguides [4] and solid breeding materials for tritium release in nuclear reactors [1–6]. In particular, lithium disilicate ( $Li_2Si_2O_5$ ) also has biomedical applications, exhibiting notable mechanical properties applicable in dentistry, as a high-strength and machinable glass ceramic [3–7]. It is also used as a substrate in storage media [8].

Lithium disilicate glass ceramics have three major phases: an orthorhombic (space group Ccc2) stable form, an orthorhombic (Pbcn) metastable form and a monoclinic (C1c1) form [4–9]. Many authors have noted that the monoclinic (C1c1) phase has very similar lattice parameters to the orthorhombic (Ccc2) form [10–13]. This is the main reason why researchers have mostly concentrated on two significant phases (metastable and orthorhombic), considering the fact that both structures have similar cell parameters, in addition to the discrepancies in diffraction peak intensities between experimental and theoretical structures [10–13].

A detailed understanding of the structural, electronic and mechanical properties of  $\text{Li}_2\text{Si}_2\text{O}_5$  is desirable for its many technological applications. In this work, we explore the aforementioned properties of monoclinic  $\text{Li}_2\text{Si}_2\text{O}_5$  using density functional theory (DFT) calculations.

2 Methodology All DFT calculations were carried out using CASTEP [14]. The convergence thresholds between optimisation cycles used were a total energy change of  $5 \times 10^{-6}$  eV/atom, with maximum force, stress and atomic displacements of  $10^{-2} \text{ eV Å}^{-1}$ ,  $2 \times 10^{-2} \text{ GPa}$ and  $5 \times 10^{-4} \,\text{Å}$ , respectively. A selection of exchangecorrelation functionals were employed, including the generalised gradient approximation (GGA) of Perdew, Burke and Ernzerhof (PBE), the revised Perdew, Burke and Ernzerhof (RPBE), Perdew Wang (PW91) and PBE with Wu-Cohen (WC) [15–18]. A Γ-centred Monkhorst-Pack scheme [19] was used to sample the Brillouin zone during the geometry optimization and mechanical property calculations. A custom k-point set of  $5 \times 5 \times 6$  was used to calculate the total and projected density of states in the primitive representation of monoclinic Li<sub>2</sub>Si<sub>2</sub>O<sub>5</sub>. Pseudo atomic functions for Li-2s<sup>1</sup>, O-2s<sup>2</sup> 2p<sup>4</sup> and Si-3s<sup>2</sup> 3p<sup>2</sup> in the

<sup>\*</sup>Corresponding author: e-mail minh.nguyen@kuleuven.be

<sup>\*\*</sup> e-mail yzulueta@uo.edu.cu, Phone: +53-22-632262, Fax: +53-22-632267

15213951, 2017, 10, Downloaded from https://onlinelbtrary.witey.com/doi/10.1002/psbs.201701018 by Egyptian National Si. Network (Ensireine), Wiley Online Library on [12032023], See the Terms and Conditions (https://onlinelbtrary.wiley.com/rerms-and-conditions) on Wiley Online Library for rules of use; OA articles are governed by the applicable Centwice Commons.

reciprocal representation were employed. The plane-wave energy cut-off, adopted for standard norm-conserving pseudopotentials, was  $550 \,\text{eV}$ . The orthorhombic Ccc2 phase is calculated to be  $0.29 \,\text{eV}$  per formula unit more stable than the monoclinic C1c1 phase.

## 3 Results and discussion

**3.1 Structural parameters** The Li<sub>2</sub>Si<sub>2</sub>O<sub>5</sub> structure consists of a combination of lithium ions tetrahedrally coordinated by oxygen and layers of the [SiO<sub>4</sub>] network, with three bridging oxygen ions per [SiO<sub>4</sub>] tetrahedron. The lithium ions occupy regions between the silicon oxygen layers. Monoclinic Li<sub>2</sub>Si<sub>2</sub>O<sub>5</sub> has lattice parameters of  $a = 5.82 \, \text{Å}$ ,  $b = 14.66 \, \text{Å}$  and  $c = 4.79 \, \text{Å}$ , resulting in a unit cell volume of 408.69 Å<sup>3</sup>, as determined by X-ray diffraction [9].

As could be expected, the lattice parameters calculated and compiled in Table 1 are somewhat over/underestimated for all exchange-correlation functionals. For monoclinic  $\text{Li}_2\text{Si}_2\text{O}_5$ , the GGA+RPBE approach produces the most accurate structure with respect to experiment. Biskri et al. [5] reported the lattice parameters of the stable orthorhombic phase using ultrasoft pseudopotentials, with the local density approximation and PBE approaches, as opposed to the norm-conserving pseudopotentials used in the present work. They found that the LDA and PBE underestimate and overestimate the lattice parameters, respectively. Our DFT calculations using GGA+RPBE reproduces the lattice parameters better than in Biskri et al. [5].

**3.2 Electronic structure** The electronic structure of monoclinic  $\text{Li}_2\text{Si}_2\text{O}_5$  was obtained using the aforementioned setup for the DFT calculations. On the basis of it giving the best agreement with experiment, the GGA+RPBE approach was used for further calculations. Fig. 1 displays the band structure of monoclinic  $\text{Li}_2\text{Si}_2\text{O}_5$ . Monoclinic  $\text{Li}_2\text{Si}_2\text{O}_5$  has a large indirect band gap of 4.98 eV near the Fermi level (0 eV), which reveals that this material has an insulating nature in the C1c1 phase. Similar electronic behaviour was reported for the Ccc2 space group [7], with a band gap of close to 5 eV [3–5].

To further explore the electronic nature of this compound, the projected and total density of states (DOS) are also calculated and shown in Fig. 2. The DOS displays three main regions. The first region (lower than  $-15\,\text{eV}$ ) is mainly dominated by O s states. The second region is the valence band that is dominated by O p and

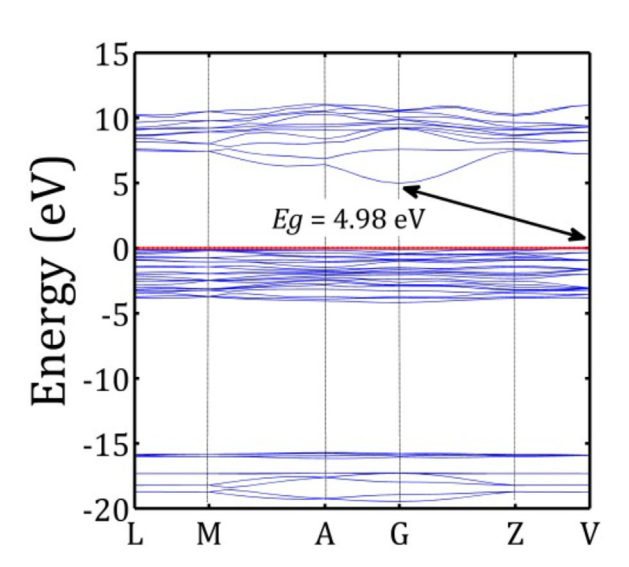


Figure 1 Band structure of monoclinic Li<sub>2</sub>Si<sub>2</sub>O<sub>5</sub>.

Si s and p, and Li s states. The last region, the conduction band, is mainly dominated by O s and p, and Si s and p states, with a lower, but not insignificant contribution, of the Li s states. The results for the valence and conduction bands confirm the existence of tetrahedral hybridisation of the SiO<sub>4</sub> framework. Similar findings were reported for orthorhombic Li<sub>2</sub>Si<sub>2</sub>O<sub>5</sub> [4, 5].

**3.3 Population analysis** Population analysis is performed using the Mulliken formalism [20]. This procedure can be used to obtain the partial charge of every atom and this procedure is widely used to explore quantities, such as atomic charge, bond population and charge transfer [3, 20–22]. The method is based on the linear combination of atomic orbitals and therefore the wave function of the system in general.

The atomic charges of each ion are listed in Table 2. As can be seen, the Li partial charge is near its formal (valence) charge. There are three oxygen ion environments in  $\text{Li}_2\text{Si}_2\text{O}_5$ . The first is labelled as O1 where oxygen ions bond to only one silicon ion. Oxygen ions bonded to two silicon ions are labelled as O2 and O3. The main difference between O2 and O3 ions is the Si–O bond length, with bond lengths of Si–O1, Si–O2 and Si–O3 being 1.55, 1.60 and 1.64 Å, respectively.

The degree of ionic character of bonding between two atoms (A and B) can be estimated by the bond ionicity  $(\mu)$ , defined as:

Table 1 Calculated lattice parameters for monoclinic Li<sub>2</sub>SiO<sub>5</sub>. The error with respect to experiment is given in brackets.

	PBE	RPBE	PW91	WC	Ref. [9]
a (Å)	5.87 (+0.86%)	5.88 (+1.01%)	5.87 (+0.86%)	5.89 (+1.01%)	5.82
b (Å)	14.53 (-0.89%)	14.54 (-0.83%)	14.50 (-1.01%)	14.54 (-0.83%)	14.66
c (Å)	4.49 (-6.26 %)	4.56 (-4.80%)	4.48 (-6.47%)	4.36 (-8.98%)	4.79



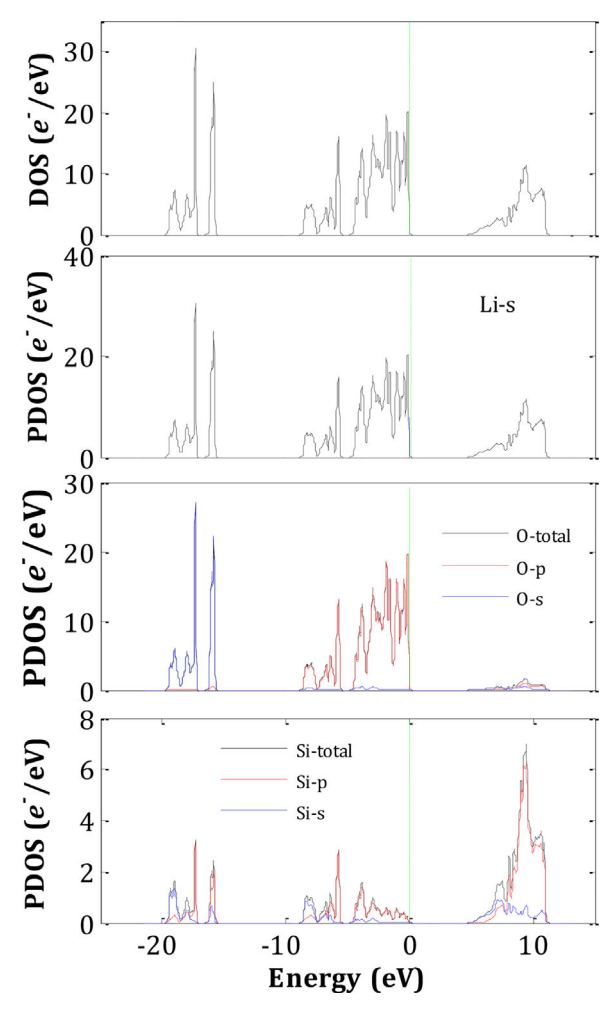


**Figure 2** Total and projected density of states of monoclinic Li<sub>2</sub>Si<sub>2</sub>O<sub>5</sub>.

$$\mu_{A-B} = \frac{1}{2} \left| \frac{q_A}{v_A} - \frac{q_B}{v_B} \right| \tag{1}$$

where  $v_A$  and  $v_B$  represent the valence (formal) charge of atoms A and B, respectively. With the partial charges compiled in Table 2, the values of  $\mu_{Si-O}$  are obtained. A value of 0.06375 for the Si-O1 bond and 0.03125 for the Si-O2 and Si-O3 bonds are obtained, consistent with the tetrahedral hybridisation of the SiO4 framework discussed

**Table 2** Atomic charges of monoclinic  $Li_2Si_2O_5$  obtained from Mulliken population analysis.

species	S	p	total	charge
Li	0.02	0.00	0.02	0.98
Si	0.61	1.22	1.83	2.17
O1	1.87	5.47	7.34	-1.34
O2	1.79	5.42	7.21	-1.21
O3	1.80	5.41	7.21	-1.21

in the PDOS analysis. Oxygen atoms in the Si–O–Si trimer yield lower bond ionicity than oxygen ions in the Si–O framework. This result is also consistent with the orthorhombic phase [3].

**3.4 Mechanical properties and stability** The elastic constant components  $(C_{ij})$  for  $\text{Li}_2\text{Si}_2\text{O}_5$  in the C1c1 and Ccc2 space groups are given in Table 3. To mechanically stabilise any crystal structure, the condition is that its strain energy must be positive to any homogeneous elastic deformation. There are 13 independent constants along the plane y=0 for the monoclinic structure, including 12 relations to satisfy the Born criteria [23, 24]. The  $C_{ij}$  values reveal that the stability conditions are actually satisfied. To our knowledge no data exists for a comparison of the values of  $C_{ii}$  in the C1c1 space group.

The  $C_{ij}$  values of the monoclinic phase are higher than for the orthorhombic phase. Small negative values of  $C_{15}$ ,  $C_{25}$ ,  $C_{35}$  and  $C_{46}$  are found for the monoclinic phase. The lattice structure in the C1c1 space group shows an orthotropic mechanical behaviour, and has three mutually perpendicular planes of elastic symmetry, resulting in nine independent  $C_{ij}$  values, which should satisfy the necessary Born criteria [23–25]. The orthotropic material behaves as monoclinic when the transformation on the original coordinate frame is applied to each symmetry plane, obtaining as a result, constitutive equations to solve Hooke's law for monoclinic materials. When the above conditions are satisfied the material in question is known as a specially orthotropic material [26].

Bulk (B), shear (G) and Young's (E) moduli were calculated and compiled in Table 4. To our knowledge, previous studies based on DFT or experiment results, regarding the exploration of mechanical properties of the monoclinic phase, have not yet been reported. Discrepancies in the estimation of mechanical properties with respect to

**Table 3** Elastic constant tensor components (in GPa) of  $\text{Li}_2\text{Si}_2\text{O}_5$ , obtained after a full geometry optimization. The errors obtained via DFT are given in brackets and the values of the Ccc2 space group are taken from Ref. [5].

	C1c1	Ccc2
$\overline{C_{11}}$	147.46 (3.12)	109.33
$C_{12}$	71.64 (0.75)	49.87
$C_{13}$	52.58 (1.13)	32.16
$C_{15}$	-0.13(0.49)	
$C_{22}$	180.79 (1.64)	147.61
$C_{23}^{-}$	43.242 (0.78)	25.76
$C_{25}$	0.23 (0.35)	
$C_{33}$	104.88 (1.52)	142.40
$C_{35}$	-0.33(0.79)	
$C_{44}$	47.08 (0.59)	37.59
$C_{46}$	-0.01 (0.003)	
$C_{55}$	79.73 (0.36)	66.22
$C_{66}$	62.31 (0.31)	57.70

<b>Table 4</b> Bulk $(B)$ , shear $(C)$	and	Young's (E	) moduli.	compressibility (	T).	Poisson's ratios.	and anisotropy	factors of Li <sub>2</sub> Si <sub>2</sub> O <sub>5</sub> .
---	-----	------------	-----------	-------------------	-----	-------------------	----------------	---

	B (GPa)				G (GPa)		E (GPa)				
space group	Reuss	Voigt	Hill	Reuss	Voigt	Hill	x	у	z	T	
C1c1	79.28	85.34	82.31	50.92	55.54	53.23	105.79	142.35	83.99	0.1261	
	Poisson's ratios:										
	xy	yx	zx	XZ	yz	zy					
	0.307	0.413	0.298	0.375	0.206	0.121					
Ccc2		67.97 (GGA .15 (LDA)	*		50.13 (GGA 5.05 (LDA)	*		20.70 (GGA) 5.36 (LDA)	•	_	
			7	values of B/	$G, F_{\mathrm{B}}, F_{\mathrm{G}}$ a	nd $F_{\rm B}/F_{\rm G}$					

values of B/O, FB, FG and FB/FG

space group		B/G		anisotrop	y factors		A <sup>U</sup> (Ref. [29]) <sup>a</sup>
	Reuss	Voigt	Hill	$\overline{F_{ m B}}$	$F_{ m G}$	$F_{ m B}/F_{ m G}$	
C1c1 Ccc2	1.56 1.36 [5]	1.54	1.55	0.037	0.043	0.85	0.53

 $<sup>^{</sup>a}A^{U} = 5(G_{\text{Voigt}}/G_{\text{Reuss}}) + (B_{\text{Voigt}}/B_{\text{Reuss}}) - 6.$ 

experiment for orthorhombic  $\text{Li}_2\text{Si}_2\text{O}_5$  have been reported previously [7]. The main reason for these discrepancies is that neither of these structures were obtained experimentally in a single crystal, only the case of  $\text{Li}_2\text{TiO}_3$  was obtained in single crystal form [27]. In polycrystalline samples, others factors, such as porosity and grain boundaries, play an important role in the determination of mechanical properties. These conditions are difficult to account for in such simulations.

The second part of Table 4 displays the ductility and brittleness criteria calculated by the Pugh formula (B/G) [3, 28], including the degree of elastic anisotropy defined as:

$$F_{\rm B} = \frac{B_{\rm Voigt} - B_{\rm Reuss}}{B_{\rm Voigt} + B_{\rm Reuss}},\tag{5}$$

$$F_{\rm G} = \frac{G_{\rm Voigt} - G_{\rm Reuss}}{G_{\rm Voigt} + G_{\rm Reuss}}.$$
 (6)

The saddle point value, which determines a ductile or brittle material, has been evaluated to be 1.75 [28]. For lower values, the material behaves in a ductile mode whereas for upper values, it is classified as brittle. All the values of *B/G* are lower than 1.75, revealing, that the structures behave as ductile materials. Li<sub>2</sub>Si<sub>2</sub>O<sub>5</sub> is a ductile compound with respect to the volume (Reuss convention) and shape (Voigt convention) change, including the results in the Hill convention, confirming its use in dentistry as a high-strength machinable glass ceramic [4, 5, 7]. The most universal measure to quantify the mechanical anisotropy in materials was proposed by Ranganathan and Starzewski [29], and it considers the contributions from the bulk part of the elastic stiffness tensor. We use this approach to further calculate the degree of anisotropy in the

C1c1 space group. This data is not currently available for the Ccc2 space group in the literature (including Ref. [5]). Alternatively, brittleness and ductility can be established by the Frantsevich criteria [30] using the Poisson ratio, where the saddle point is 1/3 (a lower value for brittle and a higher value for ductile behaviour). The Poisson's ratios  $(v_{ij})$  compiled in Table 4 correspond to a contraction response in direction j when an extension is applied in direction i (i,j=x, j and j) [26]. Through the Poisson's ratios, it can be noted that the ductile character is accentuated instead of the brittle nature of  $Li_2Si_2O_5$  in the C1c1 space group. The fact that  $v_{ij} \neq v_{ji}$  illustrates the orthotropic nature of  $Li_2Si_2O_5$  in the C1c1 space group.

From the elastic anisotropy point of view,  $\text{Li}_2\text{Si}_2\text{O}_5$  has degree of anisotropy with respect to the shape and volume change. The elastic isotropy/anisotropy is not only deterministic for solid breeder materials, but it is also very important to determine the nature of microcrack sources and propagations in polycrystalline materials. According to our results for the electronic band structure and mechanical properties, the monoclinic phase (C1c1) can be masked by the orthotropic (Ccc2) one.

**4 Conclusions** The structural, electronic and mechanical properties of monoclinic  $\text{Li}_2\text{Si}_2\text{O}_5$  have been explored using DFT calculations. The calculated lattice parameters agree well with experiment, with particularly good agreement found for the GGA+RPBE pseudopotentials. The electronic band structure analysis denotes the insulator character of the material, characterised by the large indirect band gap near the Fermi energy of 4.98 eV.

Mechanical properties were also considered using GGA+RPBE pseudopotentials. Elastic stiffness coefficients and bulk, shear and Young's moduli were calculated.



 $\text{Li}_2\text{Si}_2\text{O}_5$  is a ductile compound with respect to volume and shape. In particular, monoclinic  $\text{Li}_2\text{Si}_2\text{O}_5$  behaves as a specially orthotropic material, meaning that an orthotropic structure appears (in mechanical behaviour) to be a monoclinic structure. Thus, the monoclinic phase of  $\text{Li}_2\text{Si}_2\text{O}_5$  can be masked by the orthorhombic (Ccc2) phase.

Acknowledgements This work was supported by the Belgian Department for Development Cooperation through the Flemish Interuniversity Council-University Cooperation for Development (VLIR-UOS) in the framework of an Institutional University Cooperation programme with Universidad de Oriente, Santiago de Cuba, Cuba.

## References

- [1] C. A. Vincent, Solid State Ion. 134, 159 (2000).
- [2] B. Zhang and A. J. Easteal, J. Mater. Sci. 43, 5139 (2008).
- [3] J. C. Du and L. R. Corrales, J. Phys. Chem. B 110, 22346 (2006).
- [4] A. Alemi, S. Khademinia, and M. Sertkol, Int. Nano Lett. 5, 77 (2015).
- [5] Z. E. Biskri, H. Rached, M. Bouchear, and D. Rached, J. Mech. Behav. Biomed. Mater. 32, 345 (2014).
- [6] W. Höland, V. Rheinberger, E. Apel, and C. van't Hoen, J. Eur. Ceram. Soc. 27, 1521 (2007).
- [7] Lithium silicate glass ceramic, US Patent 7452836 (2008).
- [8] Composition inorganique pour un support d'enregistrement d'informations, European Patent EP1772440 (2007).
- [9] V. F. Liebau, Acta Crystallogr. 14, 389 (1961).
- [10] B. H. W. S. de Jong, H. T. J. Supér, A. L. Spek, N. Veldman, G. Nachtegaal, and J. C. Fischer, Acta Crystallogr. B 54, 568 (1998).
- [11] E. D. Zanotto, J. Non-Cryst. Solids **219**, 42 (1997).
- [12] J. Deubener, J. Non-Cryst. Solids 274, 195 (2000).
- [13] W. Paszkowicz, A. Wolska, M. T. Klepka, S. Abd El All, and F. M. Ezz-Eldin, Acta Phys. Polon. A 117, 315 (2010).

- [14] M. C. Payne, M. P. Teter, D. C. Allan, T. A. Arias, and J. D. Joannopoulos, Rev. Mod. Phys. 64, 1045 (1992).
- [15] J. P. Perdew, K. Burke, and M. Ernzerhof, Phys. Rev. Lett. 77, 3865 (1996).
- [16] B. Hammer, L. B. Hansen, and J. K. Norskov, Phys. Rev. B 59, 7413 (1999).
- [17] J. P. Perdew and Y. Wang, Phys. Rev. B 45, 13244 (1992).
- [18] Z. Wu and R. E. Cohen, Phys. Rev. B 73, 235116 (2006).
- [19] H. J. Monkhorst and J. D. Pack, Phys. Rev. B 13, 5188 (1976).
- [20] R. S. Mulliken, J. Chem. Phys. 23, 1833 (1955).
- [21] K. I. Ramachandran, D. Gopakumar, and K. Namboori, Computational Chemistry and Molecular Modeling: Principle and Applications (Springer, Berlin, Heidelberg, 2008), pp. 253–255.
- [22] E. G. Lewars, Introduction to the Theory and Applications of Molecular and Quantum Mechanics (Springer, Netherlands, 2011), pp. 343–359.
- [23] J. F. Nye, Physical Properties of Crystals (Oxford University Press, Oxford, 1985).
- [24] N. X. Miao, C. Y. He, C. Z. Pu, F. W. Zhang, C. Lu, Z. W. Lu, and D. W. Zhou, Chin. Phys. B 23, 127101 (2014).
- [25] F. Mouhat and F. X. Coudert, Phys Rev. B 90, 224104 (2014).
- [26] M. P. Nemeth, An In-Depth Tutorial on Constitutive Equation for Elastic Anisotropic Materials, NASA/TM-2011-217314 (Langley Research Center, Hampton, Virginia, 2011).
- [27] K. Kataoka, Y. Takahashi, N. Kijima, H. Nagai, J. Akimoto, Y. Idemoto, and K. Ohshima, Mater. Res. Bull. 44, 168 (2009).
- [28] S. F. Pugh, Philos. Mag. 45, 823 (1954).
- [29] S. I. Ranganathan and M. O. Starzewski, Phys. Rev. Lett. 101, 055504 (2008).
- [30] I. N. Frantsevich, F. F. Voronov, and S. A. Bokuta, Elastic Constants and Elastic Moduli of Metals and Insulators Handbook (Naukova Dumka, Kiev, 1983), pp. 60–180.